remote sensing

MDPI

Article

Research on Collapse Detection in Old Coal Mine Goafs Based on Space–Sky–Earth Remote Sensing Survey

Jiayi Yao [1], Keming Han [2,*], Wu Zhu [1] and Yanbo Cao [1]

[1] School of Geological Engineering and Geomatics, Chang'an University, Weishui Campus of Chang'an University, Weiyang District, Xi'an 710000, China; 2021900368@chd.edu.cn (J.Y.); zhuwu@chd.edu.cn (W.Z.); caoyanbo@chd.edu.cn (Y.C.)

[2] CCTEG Ecological Environment Technology Co., Ltd., Beijing 100013, China

* Correspondence: hkmccri@163.com

Abstract: A considerable number of coal mines employed room and pillar mining in the last century in northern China, where the goaf remained stable for a period of time; however, with the increased exposure of coal pillars, their collapse may gradually increase. The stability assessment of these old rooms and pillar goafs is challenging due to their concealment, irregular mining patterns, and the long passage of time. The methodology developed in this study, based on "space-sky-earth" remote sensing such as InSAR to trace historical deformation, the UAV observation of current surface damage, and comparison of mining spaces, can rapidly detect on a large scale the collapse of old goafs and the trend of damage. This study is conducted with an example of a coal mine in Yulin, Northern China, where obtained quantitative surface deformation values were integrated with qualitative surface damage interpretation results, followed by a yearly analysis of the overlying rock movement in accordance with the underground coal mining process. The results show that from 2007 to 2021, corresponding surface deformation and damage occurred following mining progress. However, the room and pillar goaf areas had not undergone any surface deformation, nor had there been incidents of landslides or ground fissures; therefore, it was speculated that no roof collapse had occurred in this region. The surface deformation and damage associated with underground coal mining are complex and influenced by the coal seam occurrence, mining methods, strata lithology, terrain slope, temporal evolution, and anthropogenic modifications. These phenomena are representative of the coal mining area, and this methodology can provide a reference for similar endeavors.

Keywords: goaf of coal mines; room and pillar mining; surface collapse; InSAR; UAV; aerial photography

check for updates

Citation: Yao, J.; Han, K.; Zhu, W.; Cao, Y. Research on Collapse Detection in Old Coal Mine Goafs Based on Space–Sky–Earth Remote Sensing Survey. *Remote Sens.* **2024**, *16*, 1164. https://doi.org/10.3390/rs16071164

Academic Editors: Joaquín Escayo Menéndez, Sen Du, Feng Zhao and Jordi J. Mallorquí

Received: 28 January 2024
Revised: 15 March 2024
Accepted: 18 March 2024
Published: 27 March 2024

Copyright: © 2024 by the authors. Licensee MDPI, Basel, Switzerland. This article is an open access article distributed under the terms and conditions of the Creative Commons Attribution (CC BY) license (https://creativecommons.org/licenses/by/4.0/).

1. Introduction

Limited by the mining technology of the last century, a significant portion of mines in the Yushenfu mining area of northern Shaanxi adopted the room and pillar mining method. As coal pillars are exposed over time, weathering occurs, and accompanying rheological phenomena reduce the strength of the coal pillars. In goaf areas with low-strength coal pillars, sudden instability and destruction can occur under the influence of adjacent working faces, leading to the rapid subsidence and fracture of the roof, causing extensive collapse. The resulting instantaneous instability and pressure from the falling roof can generate hurricane-like winds and rock burst disasters, posing severe threats and risks to the safety of underground personnel and the security of mining equipment and facilities, and may even trigger a mining earthquake disaster [1–3]. Thus, revealing the disaster-causing mechanism of suspended roofs in shallow coal seam areas mined with room and pillar methods is of significant importance for the safe mining of such coal layers. The stability assessment of these old room and pillar mined-out areas poses a challenge due to their concealment, irregular mining, and the extensive time since extraction [4–6]. Although geophysical prospecting and drilling have been effective, they are inefficient.

In recent years, UAV (Unmanned Aerial Vehicles) and InSAR (Interferometric Synthetical Aperture Radar) methods have been widely applied in the study of mining subsidence in mining areas due to their advantages of wide range, full coverage, and the efficient non-contact measurement of surface deformation [7–12].

This study employs "Space-Sky-Earth" remote sensing measurements, integrating InSAR to trace historical deformations [13,14], drone observations for current surface damage morphologies [7,8], and underground mining space comparisons. This approach enables the rapid, large-scale detection of collapses and damage trends in old coal mines and void areas, thereby providing technical support for the prediction of collapses in these zones.

This paper, based on the collection, understanding, and mastery of fundamental mining conditions, presents an analysis of the key challenges and difficulties in the technology, data, and applications required for comprehensive remote sensing work in mining areas. Focused long-time series spaceborne InSAR deformation observations and current high-precision UAV flights are used to integrate quantitative surface deformation measurements with qualitative surface damage interpretation results. Subsequently, in comparison with the underground coal mining process, an annual analysis of the subsidence and rock movement is conducted. Finally, research findings, including the characteristics of pillar-type mined-out areas, the extent of surface subsidence, reclamation deformation characteristics, and insights into working methods are obtained.

2. Study Area

The study area is located northwest of Shenmu City, with convenient access to transportation, including roads, railways, and air. The coal mine covers an area of 2.7 km^2 (Figure 1). The strata of the mining area are gentle, with dips generally not exceeding 3°, overall forming a monocline structure dipping towards NW. No faults or folds have been detected within the mining area, and no fractures have been observed in adjacent mines, allowing the uninterrupted advancement of the mining face. Therefore, the geological structure of this area is classified as a simple structural type.

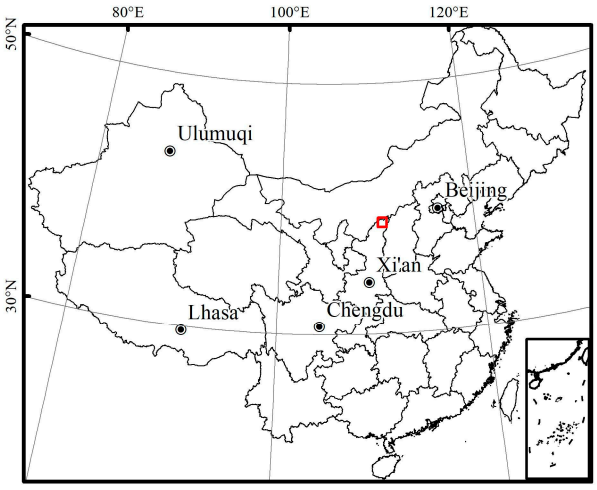


Figure 1. Location map of the study area.

The coal mine has three extractable coal seams, with mining elevations ranging from +1170 m to +995 m and a production scale of 0.6 Mt/a. The coal seams, from top to bottom, are numbered 4–2, 4–3, and 5–2. The thickness of the 4–2 seam ranges from 2.01 to 3.70 m, averaging 2.20 m; the 4–3 seam from 1.07 to 1.43 m averages 1.19 m; and the 5–2 seam from 3.42 to 4.43 m averages 3.76 m, with inter-seam distances of 20 m and 52 m, respectively. The mining sequence is 4–2 → 4–3 → 5–2. The 4–2 and 4–3 seams have been completely mined, and currently, the 5–2 seam is being exploited. The floor elevation of the 5–2 coal seam ranges from 995 to 1055 m, with a burial depth of 212 to 50 m and an average

depth of 150 m. The structure ranges from simple to fairly simple, generally without containing gangue, and the coal type is uniform, constituting a stable, thick coal seam that is extractable throughout the entire minefield. The coal is black, with a weak bituminous-to-bituminous luster, classified as semi-bright coal. The coal quality is characterized by low ash, ultra-low sulfur, low phosphorus, and an extremely high calorific value, making it a high-quality coal for power generation. It is also suitable for gasification and low-temperature dry distillation.

Prior to 2009, the majority of the 5–2 coal seams were extracted using the room-and-pillar method. The mining face adopted a method of extracting 6 m and leaving 6 m. There were three types of filling methods for the mined-out areas as follows: gangue filling, stone pillar filling, and no filling at 0.4~0.5 m. In the gangue-filled goaf, the top of the accumulated gangue was approximately 0.4 to 0.5 m from the roof of the coal chamber. The natural repose angle for the rock refuse was 35 degrees. The length of the rock refuse-filled working face generally ranged from 70 to 100 m, with an advancement length of 400 to 450 m. In the stone pillar-filled goaf, the pillars were of a regular truncated pyramid shape, with a base size of 5 m $\times$ 5 m and a top size of 4.5 m $\times$ 4.5 m. They were constructed between coal pillars along the direction of the working face advancement. The length of the stone pillar-filled working face was typically about 150 m, with an advancement length of around 450 m. The non-filling working face was located at the edges of the minefield, with a typical length of 120 to 140 m. The area of the room-and-pillar-mined voids was approximately 0.95 km^2. After 2009, longwall mining was mainly used, with full caving for managing the overlying strata.

Therefore, researching the post-mining deformation and migration patterns of the overlying rock in the 5–2 coal seam mined by the room-and-pillar method, as well as the stability of coal pillars and the dynamic evolution characteristics of pillar stress under different filling methods in the goaf, is of significant importance for the safe mining of such coal seams.

3. Technical Methods

3.1. Technical Approach

This study, based on the collection, understanding, and mastery of basic mining conditions, carries out an analysis of the key challenges in the technology, data, and applications required for comprehensive remote sensing work in the mining area. Initially, the quantitative deformation observation results were obtained from high-frequency InSAR deformation observations of Sentinel-1 C-band (150 phases) from 2016 to 2021 and low-frequency L-band InSAR deformation observations from PALSAR-1 during 2007–2011. Subsequently, qualitative surface observation results were acquired using high-precision UAV flights, obtaining a 0.5 m resolution DOM (Digital Orthophoto Map) and a 0.1 m resolution DSM (Digital Surface Model). Finally, by integrating and verifying both methods, conclusions were drawn regarding the room-and-pillar-mined voids, the range of surface subsidence, the characteristics of deformation in reclaimed areas, and an understanding of the working methods (Figure 2).

3.2. Methods

3.2.1. UAV Survey

To effectively interpret the ground fissures, ground collapse, and surface slump induced by rock movement in mined-out areas, high-resolution remote sensing images from UAV flights were used to generate detailed terrain. This allows for the detailed interpretation of surface deformation characteristics, thereby analyzing subsidence conditions in underground voids. This work uses a 1:500 scale, and the ground resolution of aerial digital images should be better than 0.05 m. The projection method uniformly adopts the Gauss–Krüger projection as a standard 3° zone planar rectangular coordinate system. The photos have a flight direction overlap of 70% and a lateral overlap of 65%. Fourteen

flight paths are set up across the entire survey area, with 62 control points, and the rotation deviation angle generally does not exceed 15°.

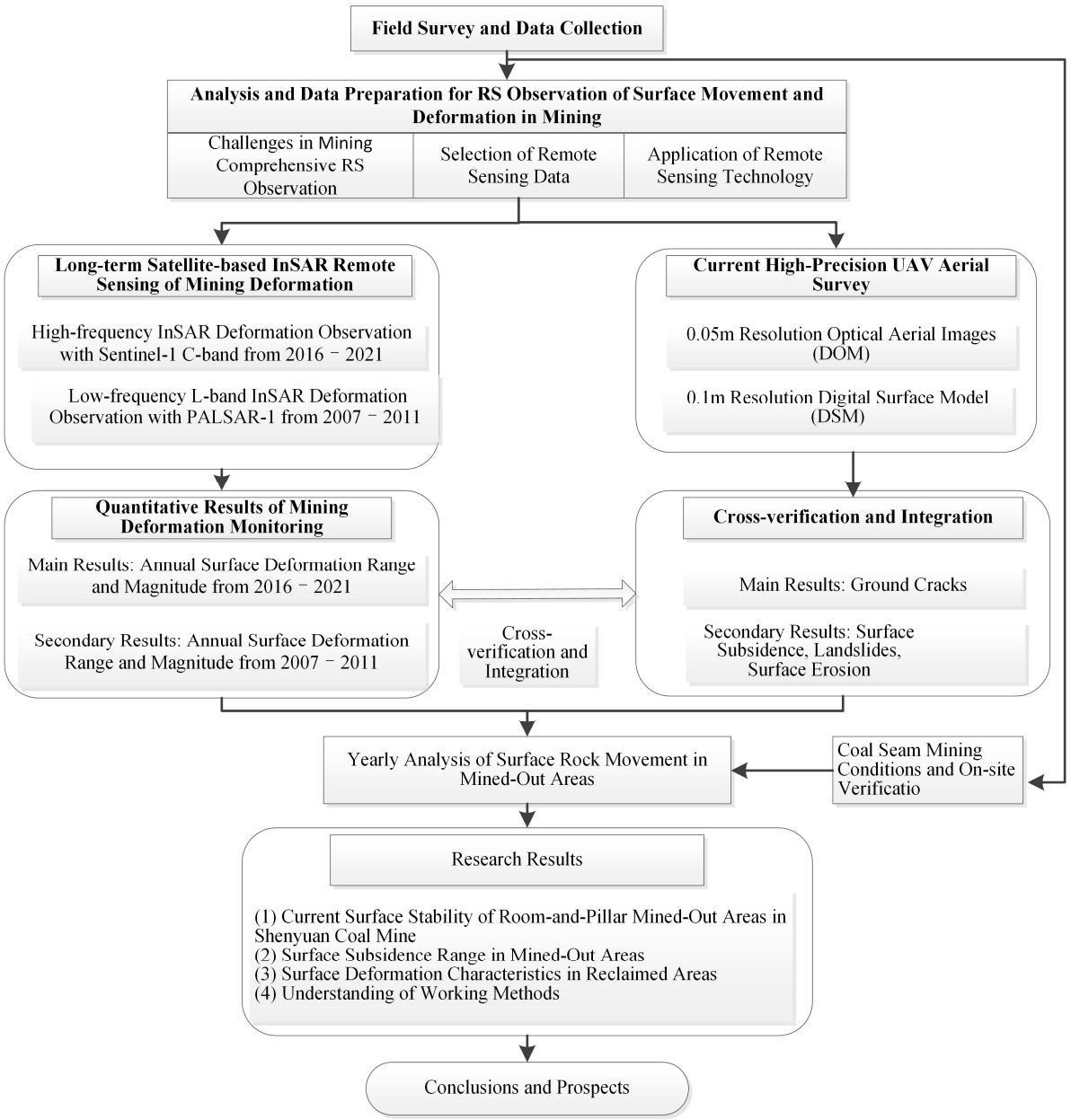


Figure 2. Technical roadmap for project implementation.

The in-house aerial survey processing uses high-precision camera posture parameters calculated by the no-ground control function to initially obtain projection information for each image. Then, the aircraft attitude data and camera parameters are optimized using an automatic extraction of corresponding points from overlapping photos and rear intersection adjustment. Subsequently, encrypted ground control points are extracted in terms of planimetry and elevation coordinates through the forward intersection of multiple cameras.

The synthesized ortho remote sensing images are clear and sharp with smooth color transitions. The quality of the completed products meets the requirements for interpreting ground fissure development. While generating optical ortho remote sensing images, high-definition topographic images with a spatial resolution of 0.1 m are also produced. As shown in Figure 3, the terrain shadow images generated from topographic data reveal that

the DSM data are of high imaging quality, clearly reflecting the geomorphic feature of the study area, which can be used for mine area topography analysis and assist in interpreting and assessing the development of ground fissures.

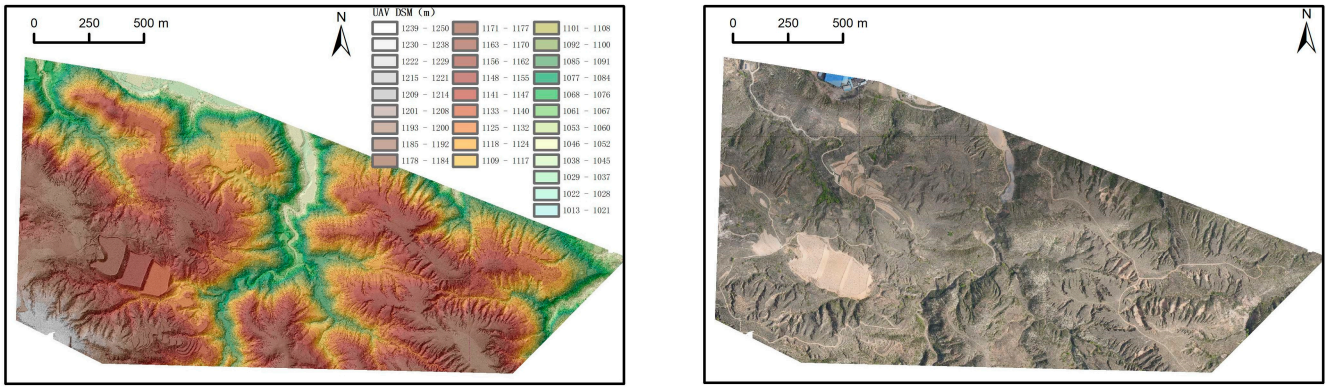


Figure 3. Ortho remote sensing images of the work area and three-dimensional landform map of the work area.

3.2.2. InSAR Deformation Observation

InSAR is a high-precision terrestrial microwave observation technique that uses repeated observations of two coherent SAR remote sensing images of the same area to form an interferometric image. It obtains surface deformation information based on the phase information of the image pixels, with a ranging principle similar to the physical double-slit interference. This paper uses two algorithms, D-InSAR and Stacking-InSAR, to calculate deformation.

D-InSAR calculations often use a "two-pass differential" method, involving calculations with two SAR images plus a Digital Elevation Model (DEM). D-InSAR results are easily affected by various errors, with theoretical accuracy generally at the centimeter level. However, it can maximally preserve the continuity and integrity of the interferometric images, effectively measuring areas with higher deformation rates and non-linear deformation zones. Further, the superimposition of multiple interferometric images (Stacking-InSAR) can reduce noise error impacts, enhance calculation precision, increase image spatial coverage, and benefit subsequent interpretation and identification.

The Sentinel-1 satellite, a C-band scientific SAR satellite launched by ESA in April 2014, offers globally free data with stable imaging, high quality, and a swath width of approximately 250 km × 250 km, making it suitable for InSAR studies. This paper utilizes ascending Sentinel-1 data coverage, starting from 15 June 2015 to June 2021, with data intervals typically of 24 or 12 days, accumulating in 152 sets of data. Three temporally adjacent datasets are used for D-InSAR interferometric calculations, totaling 408 interferometric pairs, with the maximum spatial baseline being 240.4 m and the minimum just 0.1 m (Figure 4). After completing a single D-InSAR calculation, the data are separated by year, and then the Stacking-InSAR method is used to calculate the average deformation rate for each year.

Additionally, to comprehensively detect the historical surface rock movement in the mining area, PALSAR-1 L-band data from 2007 to 2011 were used for observation. However, the data archive is not well maintained, with only three datasets available as follows: 1 July 2007, 10 October 2009, and 8 January 2011. Only D-InSAR observations can be performed with these data.

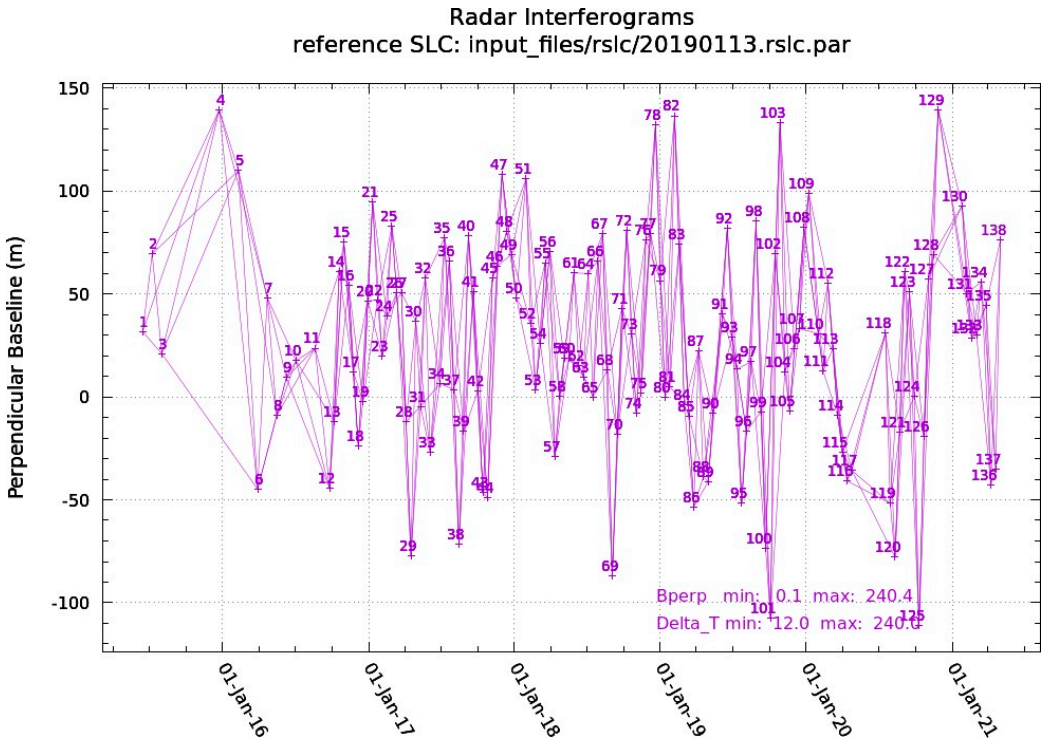


Figure 4. Spatio-temporal baseline diagram of the utilized Sentinel-1 SAR data.

4. Results and Analysis

Based on the UAV DOM and DSM in the study area and the InSAR ground deformation during two periods, 2007–2010 and 2016–2021, four types of data sources were analyzed for the current ground stability of the coal mine room-and-pillar mined-out areas, the identification of the ground subsidence range in the mined-out areas, and the analysis of ground deformation characteristics in the reclaimed areas.

4.1. Optical Interpretation

Due to the mining spanning from 2005 to 2021, including room-and-pillar, filling, and full-caving types, the ground underwent various modifications such as terracing, tree planting, crack filling, reclamation leveling, and natural erosion. Interpretation faces many challenges, including natural hazard interference, significant human modification, the long duration of mining activity, illusions caused by loess characteristics, and the significant impact of slopes on ground fissures. Therefore, interpretation followed four principles as follows: first, the principle of the on-site understanding of the characteristics of surface rock movement in the study area, given the complexity and uniqueness of geological hazards in the area, means that the on-site knowledge of the study area should be a crucial basis, and not simply copied from general geological hazard interpretation standards. Secondly, distinguishing between natural external forces and mining-induced rock movement internal dynamics means that, due to the fragile geological environment, the study area naturally develops severe collapses, landslides, and cracks near steep cliffs, which should not be interpreted as the effects of rock movement. Thirdly, distinguishing between old and new formations, as the study area has undergone over a decade of mining, with old rock movement deformation being eroded and new ones well-preserved, based on an understanding of the mining history, means that different interpretation standards should be applied in different areas; otherwise, it is difficult to interpret the richly layered and varied types of rock movement deformations, and it would be impossible to summarize these patterns later. Lastly, based on the principles of structural movement and landslide development mechanisms, underground mining rock movement is a miniaturized, accelerated version

of the structural movement process combined with landslide development, and existing structural movement patterns and phenomena can serve as references for interpretation.

To comprehensively reflect the impact of mining voids on surface rock movement, combining stratum lithology, topographical characteristics, human modification, natural erosion, and time effects, surface rock movement damage can be categorized into the following three types: ground fissures, surface landslides, and surface collapse. Due to the complexity of mining types and surface conditions in the mining area, targeted improvements are made in the interpretation process, mainly reflected in the following aspects:

(1) Optical multi-level contrast interpretation to observe the macroscopic and detailed features of fissures, landslides, and subsidence. (2) Topographic elevation and shadow overlay interpretation, considering the elevation characteristics and local details of geological disasters. (3) Topographic gravity evolution interpretation, excluding disaster phenomena occurring under natural slope gravity. (4) The dual contrast verification of optical and topographic interpretation, where both optical features and topographic characteristics match the characteristics of rock movement deformation damage. (5) Mechanical model analysis interpretation, where rock movement collapse fissures are tensile fissures typically characterized by serrated cracks, discontinuity, multiple branches, and grouped occurrence. (6) For the consideration of temporal characteristics in interpretation, generally, new fissures show more evident scarp features in the topography, while old fissures have weaker features, especially in loess-covered areas.

The interpretation results (Figures 5 and 6) show that the distribution of surface rock movement damage in the study area has certain patterns. New ground fissures and landslides are mainly distributed in the southeastern part of the mining area and are frequent and dense. The southwest part follows, with the northwest dominated by old landslides, and the central part has a few distributions, mainly suspected ground fissures and suspected filled fissures. The intensity of surface rock movement development generally correlates with the time and method of mining, with newer mining areas exhibiting stronger development. Secondly, it shows a certain correlation with the slope shape and topography, as well as the thickness of the loess and underlying strata. Field verification indicates that fissures are particularly evident in slope zones, with the phenomena of sliding along the slope being amplified.

4.2. InSAR Interpretation Results

Performing pairwise interferometry on three PALSAR-1 datasets from 2007 to 2011, D-InSAR images for July 2007 to October 2009 and October 2009 to January 2011 were generated. Despite the small amount of data and high noise, they still revealed a certain amount of deformation development in the southern region (Figure 7).

In the study area, the coherence of Sentinel-1 data varies significantly with the seasons. Interferometric quality is better in winter and spring, while it is poorer in summer and autumn, significantly affected by atmospheric conditions. In the obtained interferograms, blue areas represent stable regions, while red and yellow indicate areas of deformation.

Between 2016 and 2021, the multi-temporal Sentinel-1 data provide better interferometric results (Figure 8). The data from 2016 to 2021 cover the entire year. The 2021 SAR data end on 2 May, with most data from the winter and spring seasons providing good interferometric quality and allowing for high-quality ground monitoring results. The Stacking method, which calculates deformation through a weighted average of multi-temporal data, was used to obtain the annual average deformation for six years from 2016 to 2021 in the study area (Figure 9). Furthermore, centimeter-level surface deformation contour lines were quantitatively calculated, with deformation values corresponding to deformation phase information, showing an increase from the deformation boundary to the center. Taking the deformation from July 2020 to May 2021 as an example, the deformation zones are located in the eastern part of the mining area, with two deformation zones showing characteristics of being controlled by underground mining and influenced by local topographical features. The density and value maps of deformation contour lines drawn at 1 cm

intervals correspond well with the deformation damage characteristics interpreted from aerial imagery.

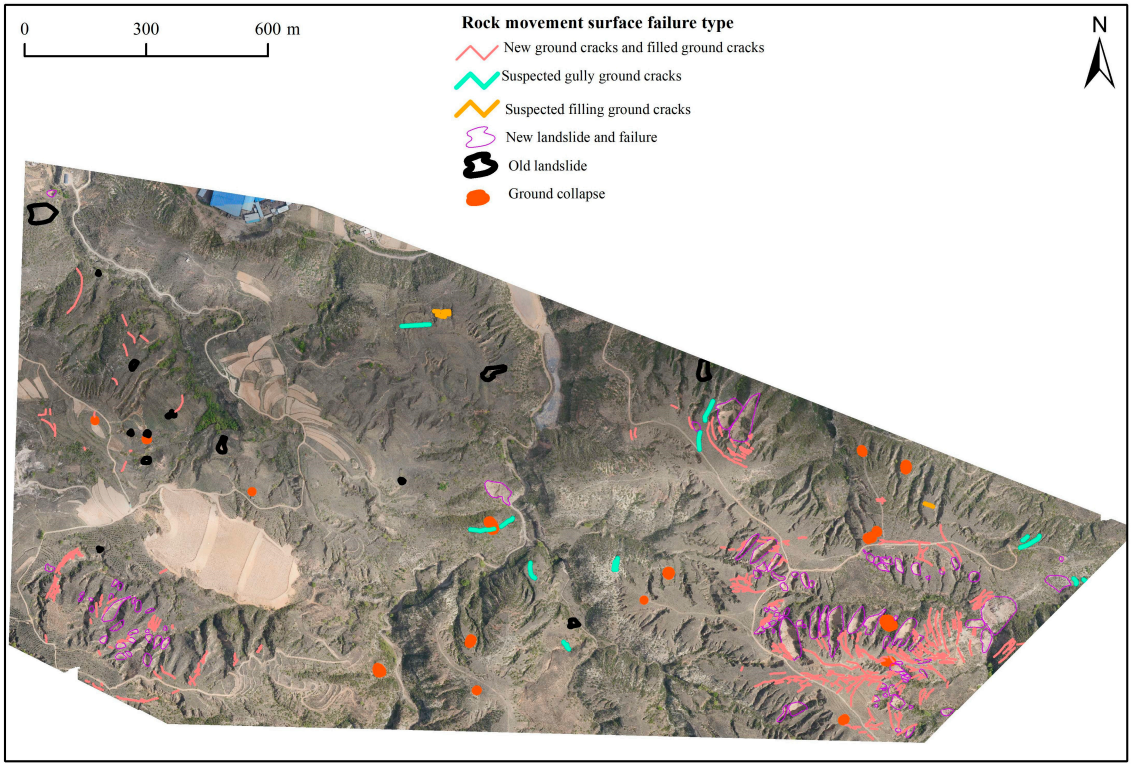


Figure 5. Interpretation results with optical aerial imagery as the background.

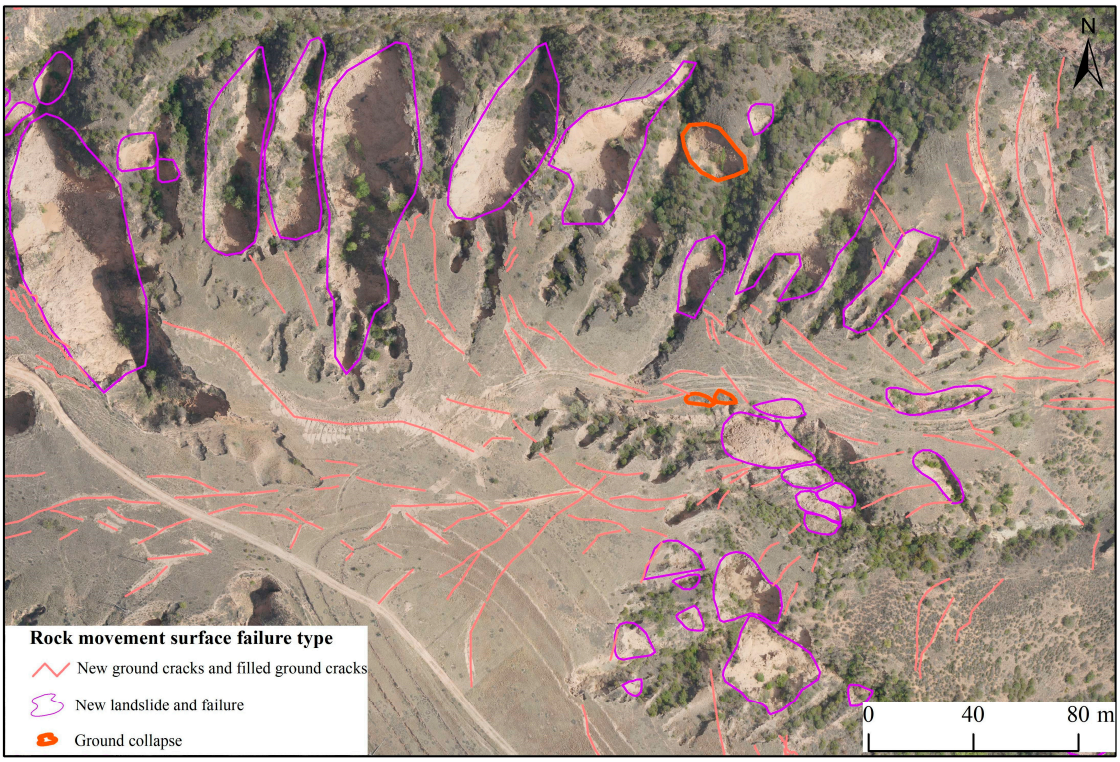


Figure 6. Interpretation of new ground fissures and landslide-dense areas in the southwest part of the mining area.

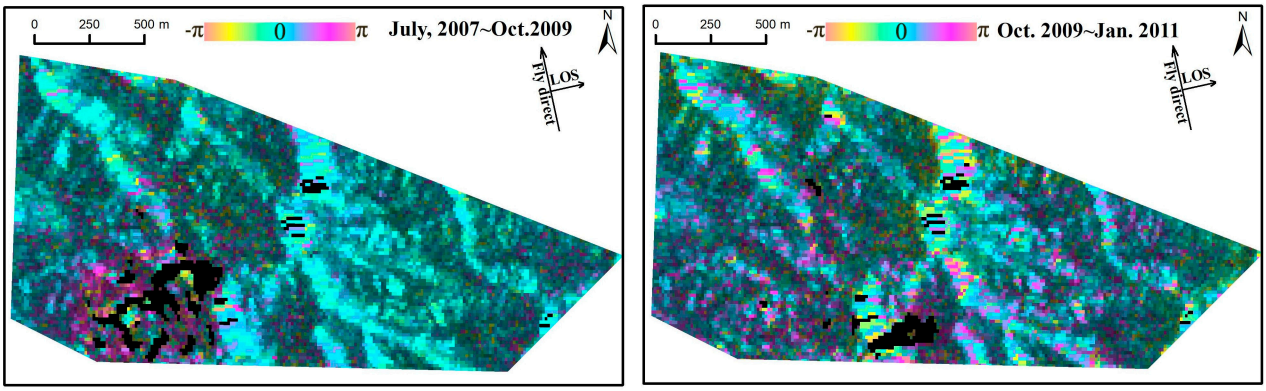


Figure 7. D-InSAR deformation map from three PALSAR-1 datasets, 2007–2010.

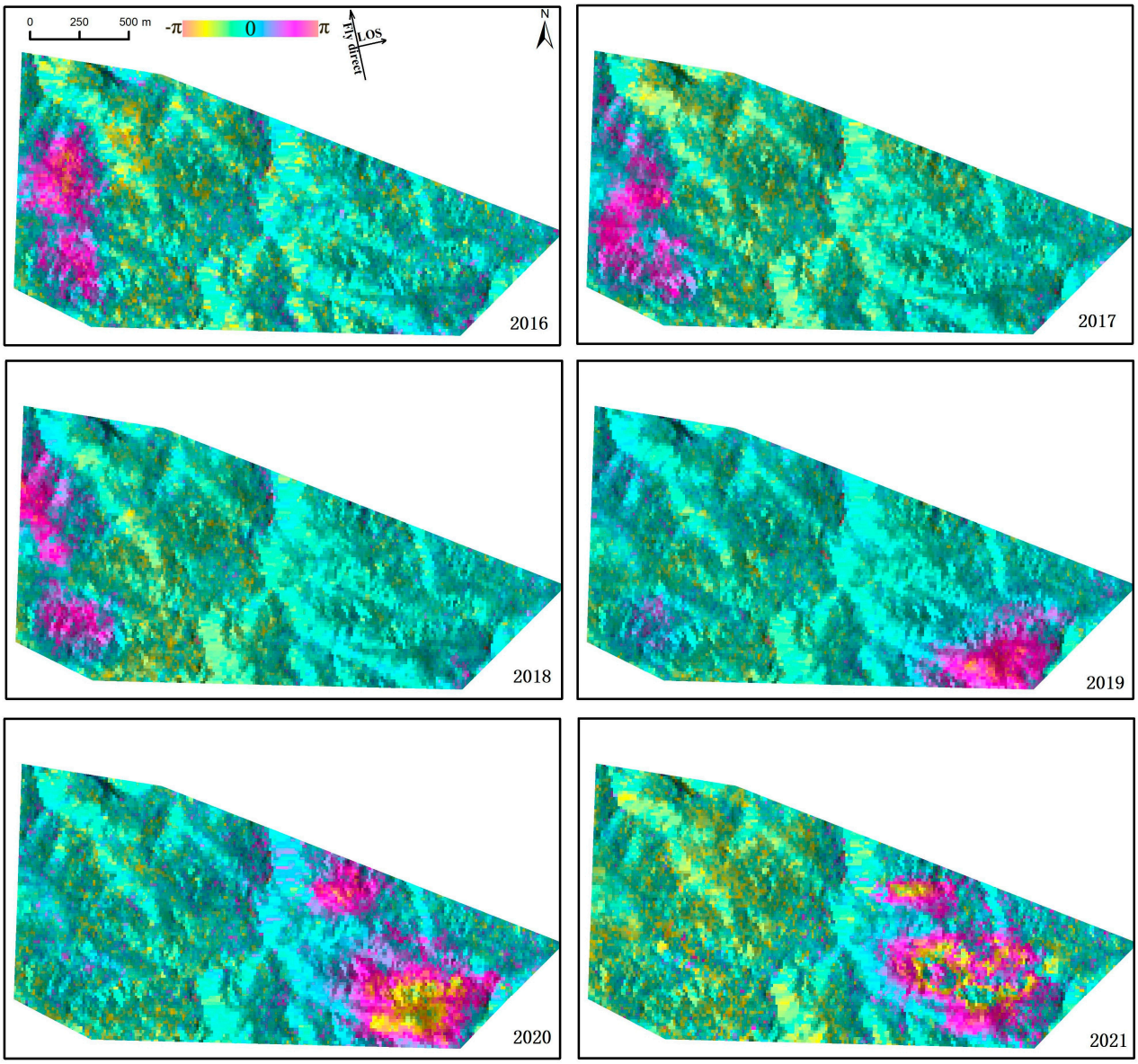


Figure 8. Annual deformation map from 2016 to 2021 Observed by Sentinel-1 data InSAR (each stripe cycle represents a deformation of 20 cm).

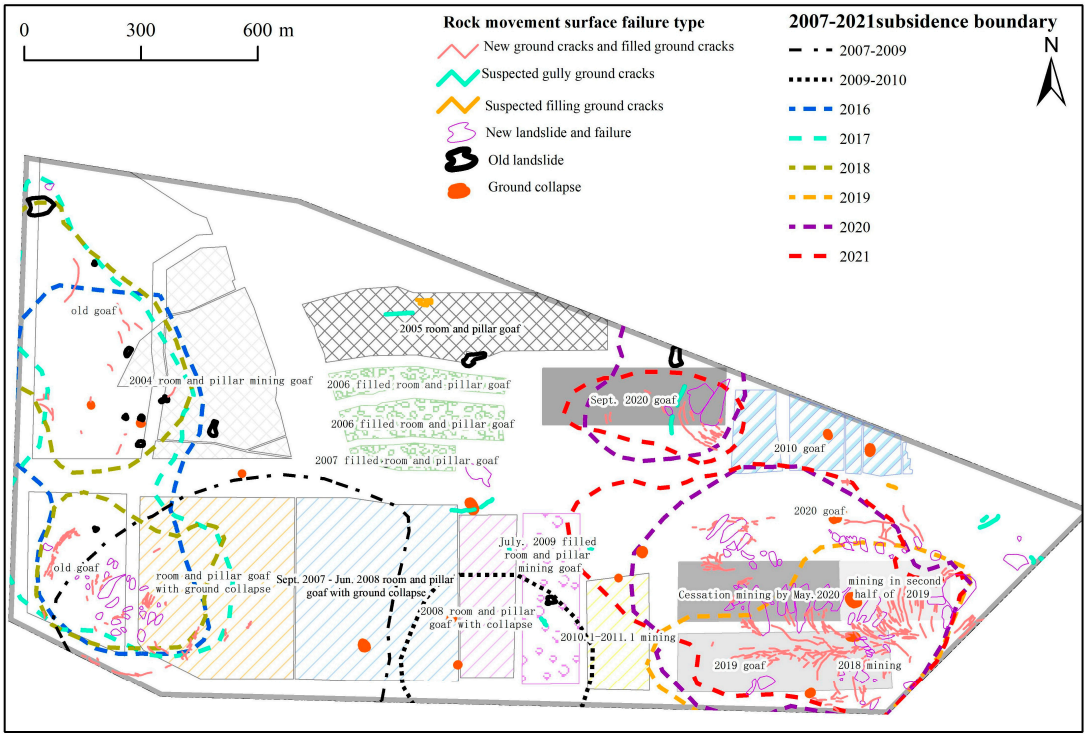


Figure 9. Relationship between underground coal mining, surface rock movement and geohazards in terms of mining time and mining type.

It should be noted that, due to the requirement of InSAR for consistent surface radar wave reflections, areas experiencing landslides, subsidence, land reclamation, or crack filling cannot be accurately measured. Therefore, InSAR deformation contour values may visually deviate from macroscopic damage deformation values observed in the field, but the overall range and deformation intensity comparison across different areas are accurate, meeting the needs for analyzing mining subsidence.

4.3. Surface Rock Movement Analysis

4.3.1. Classification of Mining Times and Types

The study area features a variety of voids and subsequent disposal types with a long history of mining. To deeply analyze the relationship between voids and surface rock movement, firstly, based on collected mining engineering plans, mining types and void times are classified into 16 categories. These include historical room-and-pillar mined-out areas that have collapsed, old mined-out areas with unknown specific years, 2004 room-and-pillar mined-out areas, 2004 room-and-pillar mined-out areas that have collapsed, 2005 room-and-pillar mined-out areas, 2006 gangue-filled room-and-pillar mined-out areas, room-and-pillar mined-out areas from September 2007 to June 2008 that have collapsed, 2007 gangue-filled room-and-pillar mined-out areas, 2008 room-and-pillar mined-out areas that have collapsed, July 2009 room-and-pillar (gangue-filled) mined-out areas, mining from January 2010 to January 2011, 2010 mined-out areas, late 2019 mined-out areas, 2019 mined-out areas, areas that stopped mining in May 2020, and mined-out areas in September 2020.

4.3.2. Impact of Mining on Surface Rock Movement

By overlaying deformation ranges from both PALSAR-1 and Sentinel-1 data over eight periods (Figure 9), significant ground deformation patterns can be observed in the study area from 2007 to 2021. From 2007 to 2011, deformation was primarily concentrated in the southwestern and southern parts. Between 2016 and 2018, deformation mainly occurred in the western part of the mining area, with no significant deformation in the east. Between

2019 and 2021, there was no significant deformation in the western part of the mining area, while deformation was concentrated in the eastern part, gradually expanding from south to north with an increasing amount of deformation each year, peaking in 2021. No significant deformation was observed in the central and north-central parts of the mining area during the InSAR observation period.

Combining coal seam distribution, the interpreted surface damage, and annual surface deformation observed by InSAR helps to organize and verify the areas of mining subsidence (Table 1). (1) Between 2007 and 2009, collapses occurred in the southern room-and-pillar mining void areas, with adjacent gangue backfill regions also experiencing some subsidence. (2) From 2009 to 2010, the southwestern room-and-pillar mining void areas underwent collapse. (3) In 2016, the western old mining areas collapsed, presumably due to the secondary deformation caused by the extraction of deep coal seams. (4) In 2017, the western mining areas extended further north from the deformation observed in 2016. (5) In 2018, the extent of deformation in the western mining areas decreased, indicating a weakening of deformation and the onset of a residual deformation phase. (6) In 2019, deformation was observed in the southeastern areas, corresponding to the comprehensive mining that began in late 2018 and continued throughout 2019, while deformation in the western areas ceased. (7) In 2020, widespread surface deformation was observed in the eastern mining areas, closely matching the underground voids created in the same year. (8) In 2021, the surface deformation in the eastern mining areas further expanded, in line with the development of coal seams. (9) Correspondingly, the deformed areas developed varying degrees of landslides, ground fissures, and surface collapses. The later the deformation occurred, the more apparent and densely distributed the damage, which is consistent with the pattern of surface weathering and erosion.

Table 1. Major surface subsidence changes over the years.

Year	Location	Area Range	Max/General Subsidence (cm/year)	Cause
2007~2009	Most of southern room-and-pillar mining area	80% middle area, 0.45 km^2	20/5	Slow, local, minor collapse of the mine roof
2009~2010	A small part of southwestern room-and-pillar mining area	50% middle area, 0.18 km^2	10/2	Slow, local, moderate collapse with borehole verification
2016	Western old mining area	Corresponding to coal seam development, 0.52 km^2	25/5	Rapid collapse synchronized with mining
2017	Western mining area further extended to the northern base on 2016 deformation area	Corresponding to coal seam development, 0.54 km^2	25/5	Rapid collapse synchronized with mining
2018	Western mining area deformation range reduced	Contraction from 2016 to 2017 deformation areas buffer, 0.42 km^2	10/4	Residual deformation after synchronous roof collapse
2019	The southeastern area	Corresponding to coal seam development, 0.33 km^2	30/8	Rapid collapse synchronized with mining
2020	Most of eastern mining area	Corresponding to coal seam development, 0.57 km^2	30/8	Rapid collapse synchronized with mining
2021	Eastern Mining Area Further expansion,	Corresponding to coal seam development, 0.58 km^2	35/10	Rapid collapse synchronized with mining

For the central-northern part of the mining area prior to 2007, no surface deformation was observed by InSAR from 2007 to 2021. The optical interpretation identified only two old landslides and three suspected ground fissures. Given the mining area's terrain with numerous gullies, steep slopes, and severe surface water erosion, these features are likely naturally developed. Therefore, it is comprehensively determined that the room-and-pillar voids from 2004 to 2005, as well as the gangue-filled room-and-pillar mining areas from 2006 to 2007, did not experience roof collapse (Figure 9).

5. Discussion

Currently, there are no dedicated standards for the interpretation of InSAR and UAV RS for surface rock movement and deformation damage in coal mine areas. The borrowed standards from surveying or geo-disaster types have weak applicability and lack significant guidance. This paper explores the principles, identification, interference information, and terrain classification for the combined interpretation of InSAR and high-resolution UAV surveys, which is a beneficial attempt.

However, a limitation is that InSAR observations primarily utilize medium-resolution Sentinel-1, the low resolution and short wavelength of which can lead to weak coherence that cannot accurately capture the time-series deformation process, only allowing for the calculation of average deformation over a period. The use of early (2007–2011) PALSAR-2 data, due to their limited quantity and long intervals, prevents multi-temporal InSAR calculations, resulting in noisy deformation maps, which are not conducive to detailed spatiotemporal deformation interpretation. Furthermore, both types of SAR data have only single-directional observation, not fully utilizing the advantages of InSAR in terms of its time series, three-dimensionality, and high-density coverage.

Optical aerial observation only has one phase of data, which is not conducive to the analysis and comparative interpretation of changes in optical and geomorphological data. The lack of traditional ground monitoring data prevents the direct and quantitative analysis and comparison of InSAR monitoring results.

This method cannot only be used for the detection of the stability and surface collapse of the room and pillar goafs but can also be applied to the localization of the goafs and the law enforcement of transboundary mining. Some scholars have developed a prototype of the underground mining detection system [15–17]. It can be seen that the use of InSAR technology combined with UAV aerial technology quickly inverts underground mining activities, and its influence has great potential.

6. Conclusions

(1) This paper presents the design of a method of coal mining old goaf collapse detection based on space–air–ground remote sensing surveying. It conducted a UAV orthophotography measurement, InSAR deformation observation, and geological interpretation through the fusion analysis of multi-source images, calculating the range and amount of surface subsidence over several years in the work area, and analyzing the current surface stability and identifying the surface collapse range of the room and pillar coal mining goaf.

(2) Influenced by coal seam occurrence, mining methods, stratum lithology, terrain slope, time evolution, and human modifications, the surface deformation and damage phenomena due to underground coal mining in the work area are complex and are representative of the Shendong area. The methods of UAV remote sensing and InSAR deformation observation used in this study can provide references for similar works.

(3) Between 2007 and 2021, as underground mining progressed in different areas, corresponding surface deformation and damage occurred, while the reclaimed surface areas showed no deformation damage.

(4) Comprehensive remote sensing observations showed that the surface of the room and pillar goaf areas from 2004 to 2005, and the areas with rock filling from 2006 to 2007 in the central and northern parts of the mining area had not experienced deformation

since 2007, with no old landslides or ground fissures, and by comparing this with the surface deformation characteristics of other mining areas, it was inferred that there had been no roof collapse in these areas.

Author Contributions: Conceptualization, J.Y.; Methodology, J.Y.; Validation, W.Z.; Investigation, J.Y.; Resources, K.H.; Writing—original draft, J.Y.; Writing—review & editing, W.Z.; Visualization, Y.C.; Supervision, K.H.; Funding acquisition, K.H. and Y.C. All authors have read and agreed to the published version of the manuscript.

Funding: This research was funded by Ministry of Science and Technology of the People's Republic of China (grant number 2022YFC3003403) and the National Natural Science Foundation of China (grant numbers 42220104005 and 41877245); CCTEG Ecological Environment Technology Co., Ltd, Special Key Projects for Sci-Tech Innovation and Entrepreneurship Fund: 2022-2-ZD004.

Data Availability Statement: The data used to support the study is available upon request to the author.

Conflicts of Interest: The Author Kenming Han was employed by the CCTEG Ecological Environment Technology Co., Ltd. The remaining authors declare that the research was conducted in the absence of any commercial or financial relationships that could be construed as a potential conflict of interest. The funders had no role in the design of the study; in the collection, analyses, or interpretation of data; in the writing of the manuscript; or in the decision to publish the results.

References

1. Peng, S.P.; Zhang, B.; Sun, X.D. *Strategic Research on Ecological Development of Closed Mines*; Science Press: Beijing, China, 2020.
2. Jin, Z.X.; Zhang, N.; Liu, W.G. *Current Status of Resource Development and Utilization of Abandoned Mines in China and Abroad*; Science Press: Beijing, China, 2020.
3. Miguel, C.C.; Hooper, A.J.; Hanssen, R.F. Surface deformation induced by water influx in the abandoned coal mines in Limburg, The Netherlands observed by satellite radar interferometry. *J. Appl. Geophys.* **2013**, *88*, 1–11.
4. Chen, B.Q.; Yu, H.; Zhang, X.; Li, Z.H.; Kang, J.R.; Yu, Y. Time-Varying Surface Deformation Retrieval and Prediction in Closed Mines through Integration of SBAS InSAR Measurements and LSTM Algorithm. *Remote Sens.* **2022**, *14*, 788. [CrossRef]
5. Chen, B.Q.; Liu, H.; Li, Z.H. Research progress and prospects on monitoring, prediction, and stability assessment of secondary subsidence in closed mines. *J. Coal Sci. Eng.* **2022**, *11*, 213–225.
6. Vervoort, A. Surface movement above an underground coal longwall mine after closure. *Nat. Hazards Earth Syst. Sci.* **2016**, *16*, 2107–2121. [CrossRef]
7. Tang, F.Q.; Lu, J.X.; Wei, S.P. Improvement of Coal Mining Subsidence Modeling Method Based on UAV LiDAR in Yushen Mining Area. *J. Coal Sci. Eng.* **2020**, *45*, 2655–2666.
8. Luo, W.; Wang, F. Coal Mine Surface Monitoring and Analysis Based on UAV Remote Sensing Technology. *J. Coal Sci. Technol.* **2021**, *49*, 268–273.
9. Tan, Z.X.; Yang, J.W.; Deng, K.Z. Research on the Method of Mining Subsidence Parameter Estimation for the Entire Mining Basin Based on SBAS-InSAR. *J. Coal Sci. Technol.* **2021**, *49*, 312–318.
10. Gueguen, Y.; Deffontaines, B.; Fruneau, B. Monitoring residual mining subsidence of Nord/Pas-de-Calais coal basin from differential and Persistent Scatterer Interferometry (Northern France). *J. Appl. Geophys.* **2009**, *69*, 24–34. [CrossRef]
11. Bu, P.; Li, C.; Liao, M. An approach for estimating underground-goaf boundaries based on combining DInSAR with a graphical method. *Adv. Civ. Eng.* **2020**, *2020*, 9375056. [CrossRef]
12. Chen, B.; Li, Z.; Yu, C. Three-dimensional time-varying large surface displacements in coal exploiting areas revealed through integration of SAR pixel offset measurements and mining subsidence model. *Remote Sens. Environ.* **2020**, *240*, 111663. [CrossRef]
13. Berardino, P.; Fornaro, G.; Lanari, R. A new algorithm for surface deformation monitoring based on small baseline differential SAR interferograms. *IEEE Trans. Geosci. Remote Sens.* **2002**, *40*, 2375–2383. [CrossRef]
14. Liao, M.S.; Wang, T. *Time Series InSAR Technology and Application*; Science Press: Beijing, China, 2013.
15. Du, S.; Wang, Y.; Zheng, M. Goaf locating based on InSAR and probability integration method. *Remote Sens.* **2019**, *11*, 812. [CrossRef]
16. Hu, Z.; Ge, L.; Li, X. An underground-mining detection system based on DInSAR. *IEEE Trans. Geosci. Remote Sens.* **2012**, *51*, 615–625. [CrossRef]
17. Xia, Y.; Wang, Y. InSAR-and PIM-based inclined goaf determination for illegal mining detection. *Remote Sens.* **2020**, *12*, 3884. [CrossRef]

Disclaimer/Publisher's Note: The statements, opinions and data contained in all publications are solely those of the individual author(s) and contributor(s) and not of MDPI and/or the editor(s). MDPI and/or the editor(s) disclaim responsibility for any injury to people or property resulting from any ideas, methods, instructions or products referred to in the content.